Article

SOURCE DATA | TRANSPARENT PROCESS

THE EMBO JOURNAL

Epigenetic reprogramming by histone acetyltransferase HAG1/AtGCN5 is required for pluripotency acquisition in *Arabidopsis*

Ji-Yun Kim[1], Woorim Yang[1], Joachim Forner[2], Jan U Lohmann[2], Bosl Noh[3,*] & Yoo-Sun Noh[1,4,**]

Abstract

Shoot regeneration can be achieved *in vitro* through a two-step process involving the acquisition of pluripotency on callus-induction media (CIM) and the formation of shoots on shoot-induction media. Although the induction of root-meristem genes in callus has been noted recently, the mechanisms underlying their induction and their roles in *de novo* shoot regeneration remain unanswered. Here, we show that the histone acetyltransferase HAG1/AtGCN5 is essential for *de novo* shoot regeneration. In developing callus, it catalyzes histone acetylation at several root-meristem gene loci including *WOX5*, *WOX14*, *SCR*, *PLT1*, and *PLT2*, providing an epigenetic platform for their transcriptional activation. In turn, we demonstrate that the transcription factors encoded by these loci act as key potency factors conferring regeneration potential to callus and establishing competence for *de novo* shoot regeneration. Thus, our study uncovers key epigenetic and potency factors regulating plant-cell pluripotency. These factors might be useful in reprogramming lineage-specified plant cells to pluripotency.

Keywords HAG1; histone acetylation; plant-cell pluripotency; SCR; WOXs
Subject Categories Chromatin, Epigenetics, Genomics & Functional Genomics; Development & Differentiation; Plant Biology
DOI 10.15252/embj.201798726 | Received 28 November 2017 | Revised 3 July 2018 | Accepted 4 July 2018 | Published online 30 July 2018
The EMBO Journal (2018) 37: e98726

See also: **N Zhang & T Laux** (October 2018)

Introduction

Plants are equipped with ability to change their cellular fate and recover their totipotency to regenerate lost parts or even reconstruct the entire organism under certain physiological conditions and environmental cues. The acquisition of totipotency and *de novo* organ regeneration can be easily monitored *in vitro* using a two-step process (Skoog & Miller, 1957). First, explants are placed on auxin-rich callus-induction media (CIM), where an intermediate form of pluripotent cell mass or "callus" is formed. Next, *de novo* shoots or roots are regenerated upon transfer of callus onto cytokinin-rich shoot-induction media (SIM) or auxin-rich root-induction media (RIM), respectively.

Due to its high regenerative potential, callus was considered an unorganized mass of dedifferentiated cells at embryonic ground state. However, recent studies have shown that the first step of callus formation involves the division of preexisting stem cells in the xylem-pole pericycle, which is also a feature of the lateral root initiation process (Atta *et al*, 2009; Sugimoto *et al*, 2010). Accordingly, *aberrant lateral root formation 4* (*alf4*) mutants, that fail to form lateral roots, cannot develop calli either (Sugimoto *et al*, 2010). Furthermore, studies using cell type-specific markers and genome-wide gene-expression profiling have revealed that root-meristem genes, such as *WUSCHEL-RELATED HOMEOBOX 5* (*WOX5*), *SCARECROW* (*SCR*), *PLETHORA 1* (*PLT1*), *ROOT CLAVATA-HOMOLOG 1* (*RCH1*), and *SHORT ROOT* (*SHR*), are highly induced upon callus formation (Atta *et al*, 2009; Sugimoto *et al*, 2010). Among them, the root stem cell regulators *PLT1* and *PLT2* are known to be required for the establishment of competence to regenerate shoot-progenitor cells (Kareem *et al*, 2015). Therefore, the formation of pluripotent callus seems to be analogous to the formation of blastema in animals where the process of trans-differentiation is required prior to regeneration (Christen *et al*, 2010; Stewart & Stankunas, 2012). However, the functional significance of the root-meristem genes in establishing pluripotent callus and the molecular mechanisms underlying their induction are yet to be elucidated.

In both mammals and plants, epigenetic modifications play pivotal roles in determining cell fate. Differentiated cells are enriched in condensed chromatin, whereas pluripotent cells display a greater amount of open chromatin enriched with active histone marks (Gaspar-Maia *et al*, 2011). The open chromatin state generally facilitates the establishment and maintenance of stem cell capacities including self-renewal and differentiation potential to various cell types (Zipori, 2004; Meshorer & Misteli, 2006; Melcer & Meshorer, 2010;

1 School of Biological Sciences, Seoul National University, Seoul, Korea
2 Department of Stem Cell Biology, University of Heidelberg, Heidelberg, Germany
3 Research Institute of Basic Sciences, Seoul National University, Seoul, Korea
4 Plant Genomics and Breeding Institute, Seoul National University, Seoul, Korea
*Corresponding author. Tel: +82 2 871 6675; Fax: +82 2 871 6673; E-mail: bnoh2003@gmail.com
**Corresponding author. Tel: +82 2 880 6674; Fax: +82 2 871 6673; E-mail: ysnoh@snu.ac.kr

Gaspar-Maia *et al*, 2011). Several studies in *Arabidopsis* suggest that the chromatin state of plants is also differentially regulated depending on cellular states (Zhao *et al*, 2001; Verdeil *et al*, 2007). However, the mechanisms and biological relevance of epigenetic controls over plant-cell pluripotency and organ regeneration remain elusive.

The *Arabidopsis* histone acetyltransferase HAG1 (Histone Acetyltransferase of the GNAT/MYST superfamily 1; Pandey *et al*, 2002), also known as *Arabidopsis thaliana* GENERAL CONTROL NONREPRESSED 5 (AtGCN5), was previously reported to affect the stem cell niche maintenance in roots by regulating *PLT1* and *PLT2* expression (Vlachonasios *et al*, 2003; Kornet & Scheres, 2009; Servet *et al*, 2010). In this study, we show that HAG1 plays a pivotal role in the establishment of pluripotency in callus and subsequent shoot regeneration. HAG1 reprograms the epigenetic status of several root-meristem genes through histone acetylation and thus activates their transcription on CIM. By yet-to-be-known mechanism, the transcription factors encoded by the root-meristem genes act as potency factors conferring competence to callus and finally allowing successful shoot regeneration subsequently on SIM. Our work reveals that HAG1-catalyzed histone acetylation acts as an epigenetic switch that renders somatic cells to acquire regeneration potential and provides a molecular mechanism underlying *de novo* shoot regeneration. HAG1 and potency factors described in this work might be useful for induced pluripotency in plants, and our results suggest a way to break the bottleneck of regeneration in plant genome engineering (Ledford, 2016).

Results

Mutations in *HAG1* cause severe defects in *de novo* shoot regeneration

Because epigenetic reprogramming is a general strategy for cell differentiation and dedifferentiation in eukaryotes, we surveyed a collection of *Arabidopsis* epigenetic mutants in our research group for their phenotypes in callus formation and organ regeneration. Among them, the *hag1-6* mutant was noted in the initial screen for its severe defect in shoot regeneration. For more careful examination of the role of HAG1 in *de novo* organ regeneration, we then used two T-DNA insertion mutants of *HAG1* and tested for their ability to regenerate roots and shoots. Both *hag1-6* and *hag1-7* mutants were capable of regenerating roots when explants pre-incubated on CIM were transferred onto the root-induction media (RIM; Fig 1A). However, *de novo* shoot regeneration was severely impaired in both mutants when CIM pre-incubated explants were transferred onto SIM (Fig 1A, and Appendix Fig S1A and B). An overexpression of FLAG-tagged HAG1 (*35S::FLAG:HAG1 hag1-7*) and an introduction of HA-tagged HAG1 under its native promoter (*HAG1:HA*; *pHAG1::HAG1:HA hag1-6*) fully rescued the shoot-regeneration defects of *hag1-7* and *hag1-6*, respectively (Fig 1A and Appendix Fig S1B). The shoot-regeneration defect of *hag1-6* was also observed when explants derived from aerial organs such as cotyledons and hypocotyls were used (Appendix Fig S1C and D). As cytokinin is well known to be essential for proper shoot regeneration, we tested whether the defect of *hag1-6* could be rescued with elevated levels of exogenous cytokinin. However, unlike wild type (WT; Col), *hag1-6* calli were not able to regenerate shoots even on media with increased cytokinin-to-auxin ratios (Fig 1B). *hag1-6* calli grew faster than WT calli and seemed to have abnormal texture and color (Fig 1C). Consistent with the faster growth, the expression of the M/G2-phase marker *CYCB1;1* (Colón-Carmona *et al*, 1999) in callus was higher in *hag1-6* than WT (Fig 1D and Appendix Fig S1E), indicating accelerated mitotic divisions in *hag1*.

Global gene-expression profiling reveals distinct expression dynamics in *hag1* calli

As a way to investigate the role of HAG1 in *de novo* shoot regeneration, we studied the global gene-expression profiles of WT and *hag1-6* in the course of *de novo* shoot regeneration by RNA-seq (Appendix Fig S1F and Dataset EV1). First, we analyzed the numbers of differentially expressed genes (DEGs) during the transition from roots to calli (R vs. C), from calli to developing shoot-progenitor cells (C vs. S), and from shoot-progenitor cells to visible shoots (S vs. S2W) (Fig 1E and Dataset EV2). In WT, the largest number of DEGs was found in the R vs. C comparison (3,783 upregulated and 3,284 downregulated genes), indicating a global gene-expression change during the R to C transition. A smaller number of genes were differentially expressed during the C to S transition (556 upregulated and 875 downregulated genes), suggesting that the

Figure 1. Mutations in *hag1* cause severe defects in *de novo* shoot regeneration.

A Callus, *de novo* shoot, and root formation in wild-type (WT; Col), *hag1-6*, *hag1-7*, and *35S::FLAG:HAG1 hag1-7* root explants. Root explants were transferred onto CIM for 1 week and then transferred onto fresh CIM, SIM, or RIM for callus, *de novo* shoot, or root induction, respectively. Scale bar: 1 cm. Graph on the right shows the percentage of explants with shoots formed as scored at 18 days on SIM. 36 explants of each genotype were used for scoring.

B Shoot regeneration assay using Col and *hag1-6* root explants on media with different cytokinin (2IP) to auxin (IAA) ratios. Col and *hag1-6* root explants derived from 20 seedlings were first incubated on CIM for 2 weeks and then transferred onto 150 mg/ml IAA-containing media supplemented with 0, 500, or 5,000 mg/ml 2IP. Pictures were taken at 27 days after transfer onto each media using representative explants. Scale bar: 2 mm.

C Root explant-derived calli of Col and *hag1-6* at 4 weeks on CIM (left). Scale bar: 1 mm. 4-week-old calli derived from 30 seedling roots of each genotype were collected to measure callus fresh weight (right).

D Histochemical GUS staining of *CYCB1;1:GUS* in Col (left) and *CYCB1;1:GUS* in *hag1-6*. Shown are root explants at 4 days on CIM. Scale bar: 1 mm. See Appendix Fig S1E for GUS signal quantification.

E Statistic chart of differentially expressed genes (DEGs) in Col and *hag1-6* roots (R), 4-day CIM-incubated root explants (C), 4-day CIM-incubated + 2-day SIM-incubated root explants (S), and 4-day CIM-incubated + 2-week SIM-incubated root explants (S2W). Green: upregulated genes, $\log_2$ ratio ≥ 1; red: downregulated genes, $\log_2$ ratio ≤ -1; FDR < 0.01.

F Immunoblot analysis of HAG1:HA protein. Samples are as described in (E). One-week CIM-incubated Col root explants (Col) were used as negative control. Ponceau staining was performed as loading control.

Data information: In (A and C), data are presented as means ± SE. Student's *t*-test (two-tailed) $*P \leq 0.001$, $**P \leq 0.01$.
Source data are available online for this figure.

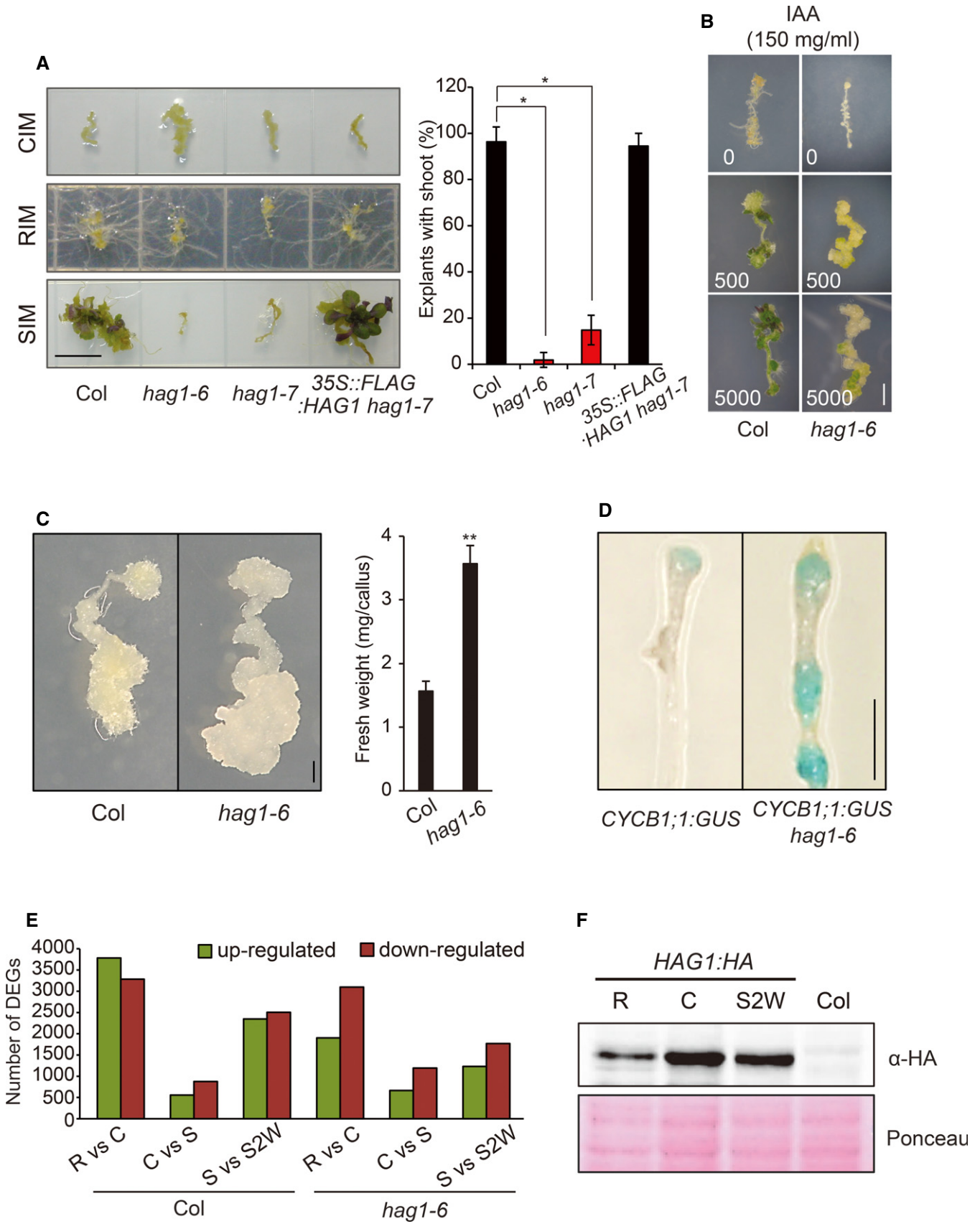

Figure 1.

process of early shoot regeneration might accompany differential expression of a subset of phase-specific genes. In *hag1*, the overall number of upregulated genes was smaller than in WT (6,688 in WT vs. 3,859 in *hag1-6*). Importantly, the ratio of downregulated genes to upregulated genes, especially during the R to C transition, was higher in *hag1* than in WT: While 3,783 and 3,284 genes were upregulated and downregulated, respectively, in WT, 1,963 and 3,097 genes were upregulated and downregulated, respectively, in *hag1* during the R to C transition. The increased proportion of downregulated DEGs in *hag1* is well correlated with the general role of HAG1 as a positive regulator of transcription.

Next, we analyzed a group of genes that showed constant expression at all time points (unchanged expression; UC) in WT and *hag1* (Appendix Fig S1G and H, and Dataset EV3). The number of UC genes was higher for *hag1* (1,002 genes) than WT (652 genes; Appendix Fig S1G). Further, a substantial number of the UC genes (388) were specific to *hag1* (Appendix Fig S1H and Dataset EV3). We then classified these *hag1*-specific UC genes based on their expression patterns in WT (Appendix Fig S1I and Dataset EV4). Interestingly, the largest portion of these genes (64.4%) was upregulated during the R to C transition in WT (Appendix Fig S1I), indicating that many genes upregulated during callus formation in WT are not induced in developing *hag1-6* calli. Conversely, expression of the majority of the *hag1*-specific UC genes (88.4% or 55.9%) was unchanged during the C to S or S to S2W transition in WT, respectively, suggesting that HAG1 is unlikely to play a major role during these steps (Appendix Fig S1I and Dataset EV4). Consistently, the induction of genes involved in the establishment of shoot stem cell niche, such as *WUSCHEL* (*WUS*) and *CUP-SHAPED COTYLEDON 2* (*CUC2*; Laux *et al*, 1996; Mayer *et al*, 1998; Gallois *et al*, 2002, 2004; Motte *et al*, 2011; Kareem *et al*, 2015), was not affected by the *hag1-6* mutation on SIM (Table EV1). However, the expression pattern of *WUS* in *hag1-6* callus on SIM was distinct from that in WT callus (Appendix Fig S2A). In contrast to the localized *WUS* expression in the callus cells peripheral to the shoot-meristem progenitors in WT (Gordon *et al*, 2007), *WUS* expression in *hag1-6* was dispersed throughout the callus at 5 and 7 days on SIM and was not detected later at 12 days, reflecting the failure of *de novo* shoot-meristem formation.

In sum, the RNA-seq analysis indicated a massive gene-expression change and a critical role of HAG1 during the R to C transition. The failure of HAG1 target-gene induction on CIM subsequently causes mispatterning of the major shoot-meristem maintenance factor WUS on SIM. Consistent with the major role of HAG1 on CIM, the expression level of HAG1 protein was increased during the R to C transition (Fig 1F). Based on these results, we hypothesized that the main role of HAG1 on CIM might be in the activation of genes encoding potency factors that confer pluripotency to cells in callus and thus competence for *de novo* shoot regeneration subsequently on SIM.

Expression of *WOX5*, *SCR*, *PLT1*, and *PLT2* in calli is severely reduced by *hag1* mutation

Our RNA-seq data revealed that the expression of several genes known to be involved in root-meristem establishment or maintenance is induced on CIM in WT explants as previously reported (Sugimoto *et al*, 2010) but, notably, not in *hag1* explants (Table EV1). Among them, the expression of *WOX5*, a quiescent center (QC)-specific gene crucial for root stem cell maintenance, remained low at all stages in *hag1* (Appendix Fig S3A). The *WOX5*-promoter activity examined by the *pWOX5::GFP-ER* transgene spread to the entire callus-forming regions in WT callus and, upon transfer onto SIM, was decreased gradually and completely absent after 7 days on SIM (Fig 2A and Appendix Fig S2B). However, in a *hag1* mutant background, the *WOX5*-promoter activity was substantially reduced at all time points observed (Fig 2A and Appendix Fig S2B). Similarly, *WOX5* transcript levels were also drastically increased in WT calli derived from aerial tissues such as hypocotyls and cotyledons, whereas these increases were not observed in *hag1* calli (Fig 2D and E).

Root stem cell niche is known to be maintained by the two parallel pathways: the SCR and PLT pathways (Aida *et al*, 2004). We noted that the transcript levels of *SCR* were significantly lowered by the *hag1-6* mutation in both CIM- and early SIM-incubated explants (Appendix Fig S3B). A closer examination of *SCR* expression by using *pSCR::GFP-ER* revealed that the *SCR*-promoter activity, which is active in the endodermis and QC in roots, is observed in the subepidermal layers of developing calli on CIM as reported previously (Sugimoto *et al*, 2010; Fig 2B and C). Upon transfer onto SIM, the *SCR*-promoter activity was decreased gradually and completely absent after 7 days on SIM (Fig 2B). In *hag1* mutant, the *SCR*-promoter activity was detected in the endodermis and QC at 1 day on CIM as in WT. However, it was reduced throughout later stages in CIM-incubated *hag1* calli compared to WT (Fig 2B and C, and Appendix Fig S2C). Next, we compared the expression of *SCR* in aerial tissue-derived WT and *hag1* calli. Decreases in *SCR* transcript levels by the *hag1-6* mutation were also observed in both cotyledon- and hypocotyl-derived explants (Fig 2F and G).

PLT1 and *PLT2* were reported to be required for the acquisition of competence to regenerate shoot-progenitor cells (Kareem *et al*,

Figure 2. *WOX5* and *SCR* expression is reduced in *hag1*.

A *pWOX5::GFP-ER* expression in Col (WT) and *hag1-6* explants on CIM and SIM. Time points selected for observation are indicated. Cellular outlines were visualized with propidium iodide (PI) staining (red).

B *pSCR::GFP-ER* expression in Col (WT) and *hag1-6* explants on CIM and SIM. Time points selected for observation are indicated. Cellular outlines were visualized with PI staining (red).

C *pSCR::GFP-ER* expression in Col (WT) and *hag1-6* root tips at various time points on CIM. Time points selected for observation are indicated. Cellular outlines were visualized with PI staining (red).

D, E *WOX5* transcript levels in Col and *hag1-6* hypocotyl (D) and cotyledon (E) explants at indicated days on CIM.

F, G *SCR* transcript levels in Col and *hag1-6* hypocotyl (F) and cotyledon (G) explants at indicated days on CIM.

Data information: Scale bars: 50 μm (A–C). In (A–C), at least 25 independent explants from each genotype were used for observation to confirm representative expression patterns of each marker in each genotype. In (D–G), data are presented as means ± SE of three biological replicates. Col levels at CIM 0 day were set to 1 after normalization with *UBQ10*. Student's *t*-test (two-tailed) $*P \leq 0.01$, $**P \leq 0.005$.

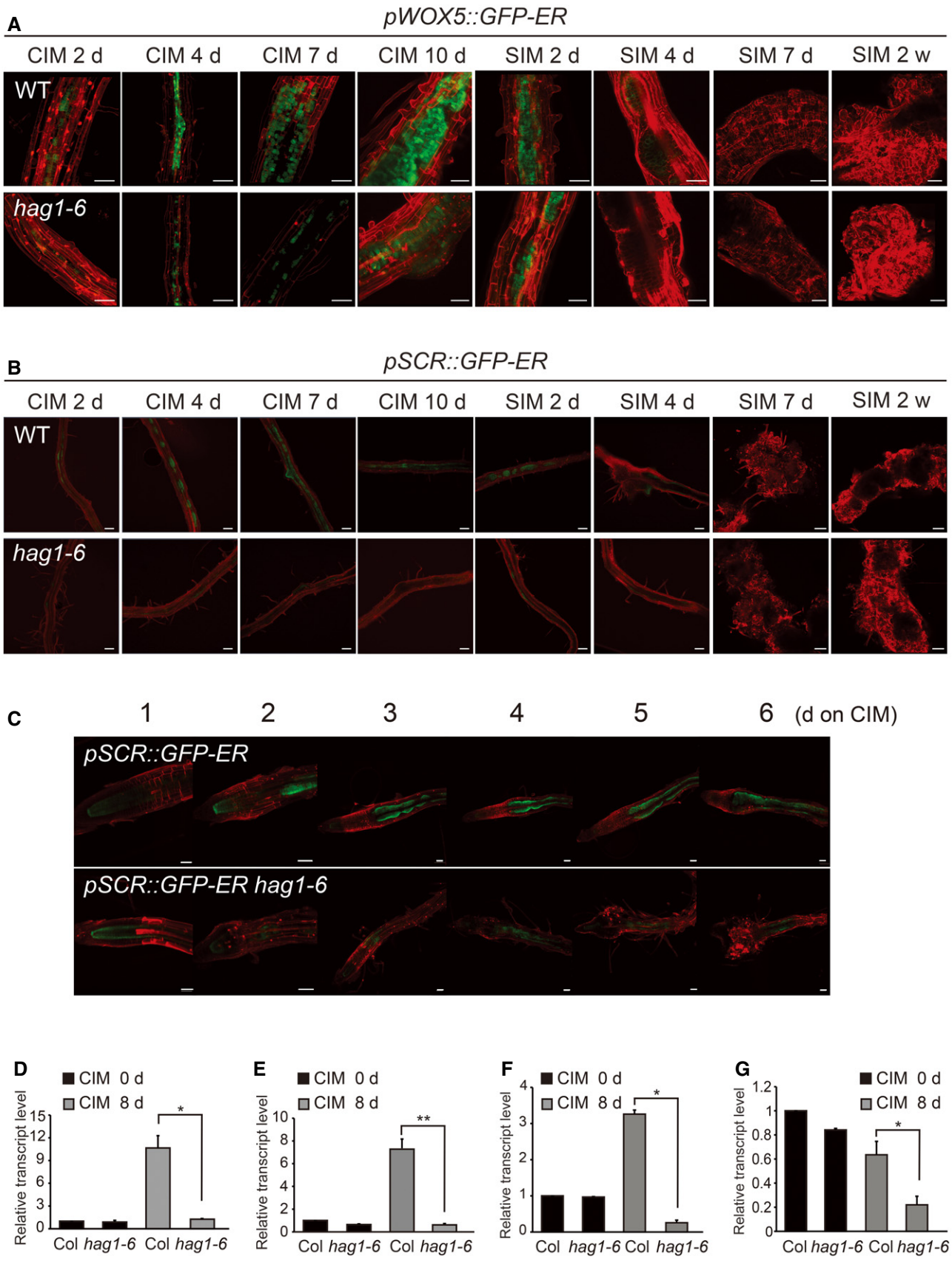
A
pWOX5::GFP-ER
CIM 2 d
CIM 4 d
CIM 7 d
CIM 10 d
SIM 2 d
SIM 4 d
SIM 7 d
SIM 2 w
WT
hag1-6
B
pSCR::GFP-ER
CIM 2 d
CIM 4 d
CIM 7 d
CIM 10 d
SIM 2 d
SIM 4 d
SIM 7 d
SIM 2 w
WT
hag1-6
C
1
2
3
4
5
6
(d on CIM)
pSCR::GFP-ER
pSCR::GFP-ER hag1-6
D
CIM 0 d
CIM 8 d
Relative transcript level
Col
hag1-6
Col
hag1-6
E
CIM 0 d
CIM 8 d
Relative transcript level
Col
hag1-6
Col
hag1-6
F
CIM 0 d
CIM 8 d
Relative transcript level
Col
hag1-6
Col
hag1-6
G
CIM 0 d
CIM 8 d
Relative transcript level
Col
hag1-6
Col
hag1-6

Figure 2.

2015). Transcript levels of *PLT1* and *PLT2* were drastically increased upon CIM incubation in the root-, hypocotyl-, and cotyledon-derived WT calli, whereas their increases in *hag1* calli were < 50% of WT (Appendix Fig S3C–H). Together, these results indicate that the shoot-regeneration defect observed in root-, hypocotyl-, and cotyledon-derived explants of *hag1* is correlated with the reduced expression of *WOX5*, *SCR*, *PLT1,* and *PLT2* during CIM incubation.

H3Ac within *WOX5*, *SCR*, *PLT1*, and *PLT2* chromatin is directly controlled by HAG1

To understand the role of HAG1 as a histone acetyltransferase in epigenome reprogramming during callus formation, we harvested 1-week CIM-incubated calli derived from WT and *hag1-6* roots and generated genomewide histone H3 acetylation (H3Ac) maps by chromatin immunoprecipitation (ChIP) followed by high-throughput DNA sequencing (ChIP-seq). H3Ac was highly enriched at the transcription start sites (TSS) in both WT and *hag1* (Appendix Fig S4A–C). In accordance with previous reports that have defined HAG1 as a gene-specific coactivator required for the expression of subset of genes rather than a global transcriptional regulator (Lee *et al*, 2000; Krebs *et al*, 2011; Bonnet *et al*, 2014), the overall H3Ac-enrichment pattern and number of H3Ac peaks of *hag1* were comparable to those of WT across all the five chromosomes of *Arabidopsis* (Appendix Fig S4A–C and Dataset EV5), although some specific loci, including *WOX5*, *SCR*, *PLT1*, and *PLT2* (Fig 3A–D, Appendix Fig S4D–G, and Datasets EV5–EV7), showed substantially lower H3Ac levels in *hag1*.

For in depth analyses of these loci, we then performed ChIP-qPCR analyses using roots and CIM-, and SIM-incubated explants of WT and *hag1-6* (Fig 3E–H). In WT, H3Ac enrichment at these loci increased upon CIM incubation with peaks around the TSS of these genes. However, in *hag1,* H3Ac levels were lower compared to WT, specifically in CIM-incubated explants. Unlike the above loci, several downstream-target loci of WOX5, SCR, or PLT1/PLT2 showed comparable H3Ac levels yet reduced expressions in *hag1* compared to WT (Appendix Fig S5A and B), suggesting that H3Ac-mediated regulation might be specific to the upstream *WOX5*, *SCR*, *PLT1*, and *PLT2* loci.

Next, we examined whether *WOX5*, *SCR*, *PLT1*, and *PLT2* are direct targets of HAG1. ChIP assays using anti-HA antibody revealed that upon CIM incubation, the HAG1:HA protein indeed associates directly with the promoters and transcribed regions of *WOX5*, *SCR*, *PLT1*, and *PLT2*, but not with the control locus *WUS* nor *Actin 2/7* (Fig 3I–L and Appendix Fig S6A–C). Notably, the targeting of HAG1:HA to these loci was detected only in CIM-incubated explants in concordance with the increased expression of HAG1 protein during CIM incubation (Fig 1F) and the lack of H3Ac increase in *hag1* explants on CIM (Fig 3E–H).

WOX5 and *WOX14* are required for pluripotency and *de novo* shoot regeneration

According to a previous report (Kareem *et al*, 2015), the *plt1 plt2* double mutant shows a reduced efficiency in *de novo* shoot regeneration and *PLT1* and *PLT2* are both required for callus to acquire competence to regenerate shoot-progenitor cells. However, it is yet to be known whether *WOX5* and *SCR* are required for *de novo* shoot regeneration. Hence, to understand the link between the reduced expression of *WOX5* and the shoot-regeneration defect of *hag1*, we obtained two T-DNA insertion mutants of *WOX5* and analyzed their shoot-regeneration phenotypes. Both *wox5-1* and *wox5-3* showed minor defects in shoot regeneration (Appendix Fig S7A and B). We reasoned that other members of the *WOX* family might possibly act redundantly with *WOX5* and then further investigated the roles of *WOX7* and *WOX14* among the 15 *WOX*-family genes as these two showed similar expression patterns with *WOX5* in WT and *hag1* (Fig 4A and B, Appendix Fig S7C, and Table EV2).

WOX7 was previously reported to play a role in integrating lateral root developmental program and sugar response in *Arabidopsis* (Kong *et al*, 2016). In our assay, *wox7-1* mutants did not show noticeable phenotypes during rosette development but displayed slightly shorter primary root length compared to WT (Appendix Fig S7D and E). WOX14 has been known to act in various aspects of plant development including GA biosynthesis, the lignification of inflorescence stems, and the promotion of procambial cell proliferation and differentiation (Etchells *et al*, 2013; Denis *et al*, 2017). *wox14-1* mutants showed shorter primary root length compared to WT as reported (Appendix Fig S7D and E) (Deveaux *et al*, 2008). Although the *wox5-3 wox7-1 wox14-1* triple mutants generated by genetic crosses also showed slightly shorter primary root length compared to WTs, an additive effect on the root length compared to each single mutants was not observed in the triple (Appendix Fig S7E).

Unlike the root phenotype, when each single and the *wox5-3 wox7-1 wox14-1* triple mutants were subjected to shoot-regeneration assays, *wox14-1* showed the strongest defect among the single mutants and *wox5-3 wox7-1 wox14-1* displayed the most severely impaired shoot-regeneration phenotype compared to any single mutants, indicating an additive effect from combining single mutations (Fig 4C and D). F1 hybrids generated by crosses between Col and No (Col × No F1) showed an intermediate shoot-regeneration efficiency compared to Col and No WTs, suggesting that the severe defect of *wox5-3 wox7-1 wox14-1* in shoot regeneration is not likely due to genetic modifiers in the accessions (Appendix Fig S7F). Therefore, unlike in primary root development, *WOX5* and *WOX14*, with minor contribution of *WOX7*, seem to have redundant roles in conferring competence for *de novo* shoot regeneration.

We then evaluated whether HAG1 also directly catalyzes histone acetylation at the *WOX7* and *WOX14* locus. H3Ac level at the *WOX7* locus in callus was slightly affected by *hag1* mutation (Appendix Fig S7G). At the *WOX14* locus, H3Ac levels were increased during CIM incubation, especially at the TSS (Fig 4E and F). However, in *hag1-6*, H3Ac levels at *WOX14* were not increased during CIM incubation and remained lower than in WT. Moreover, HAG1:HA protein enrichment at *WOX14* was detected during CIM incubation (Fig 4G). Taken together, the results above and in the previous section demonstrate that H3Ac directly catalyzed by HAG1 induces the transcriptional activation of *WOX5* and *WOX14*, two members of the *WOX*-family genes that act redundantly in conferring competence for *de novo* shoot regeneration to callus.

WOX5 and *SCR* have additive roles in the acquisition of pluripotency and competence for *de novo* shoot regeneration

As *SCR* displayed a similar expression dynamics with *WOX5* during the course of *de novo* organogenesis, we studied if *SCR* also has a role in *de novo* shoot regeneration by examining the phenotypes of two *scr*

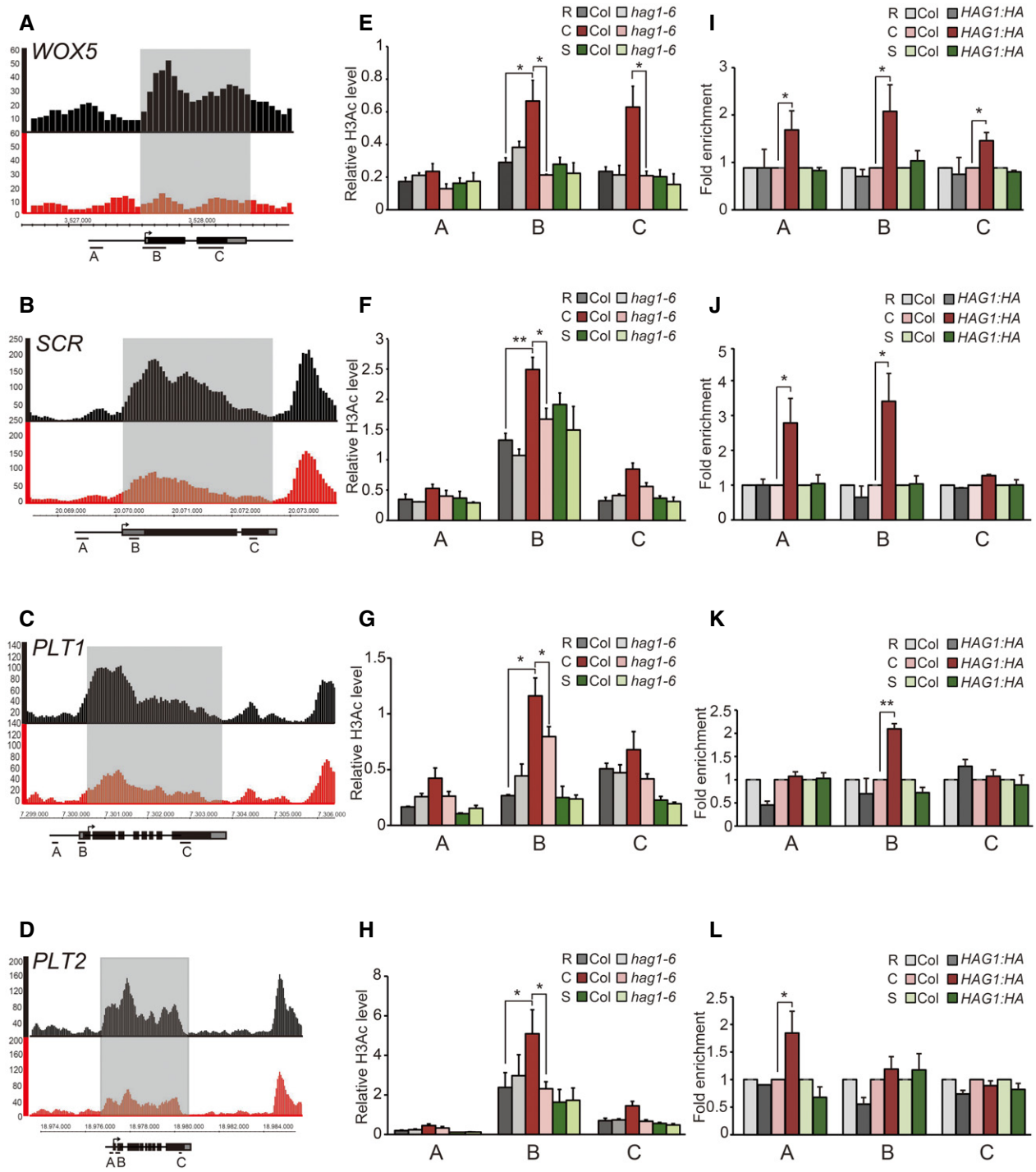

Figure 3. *WOX5*, *SCR*, *PLT1*, and *PLT2* loci are direct histone acetylation targets of HAG1.

A–D H3Ac enrichment at the *WOX5* (A), *SCR* (B), *PLT1* (C), and *PLT2* (D) loci in Col (upper black diagram) and *hag1-6* (lower red diagram) calli (1-week CIM) as determined by ChIP-seq. *P*-value cutoff for peak detection using MACS2 was $5e^{-2}$ for *WOX5* (A) and $1e^{-5}$ for *SCR* (B), *PLT1* (C), and *PLT2* (D). ChIP-seq data were visualized using Integrated Genome Browser (IGB; http://bioviz.org/igb/index.html). The *x*- and *y*-axes represent the genomic position of the corresponding gene and the number of overlapping reads per base pair position, respectively. Schematic representation of each locus is depicted at the bottom. Exons are indicated as boxes, whereas intergenic sequences and introns are marked with lines. 5′ and 3′ UTRs are represented as gray boxes. Transcription start sites are indicated with arrows.

E–H ChIP-qPCR analysis of H3Ac levels at the *WOX5* (E), *SCR* (F), *PLT1* (G), and *PLT2* (H) loci in Col and *hag1-6*. Root (R), 1-week CIM (C), and 1-week CIM + 2-week SIM (S) samples were used for assays. Regions tested are indicated in the schematics in (A–D).

I–L Direct targeting of HAG1:HA protein to *WOX5* (I), *SCR* (J), *PLT1* (K), and *PLT2* (L) chromatin as determined by ChIP-qPCR. Samples were prepared as described in (E–H).

Data information: Data are the means ± SE of three biological replicates as relative values to *UBQ11* after normalization to input DNA (E–H) or the means ± SE of three biological replicates obtained after normalization to input DNA (I–L). Student's *t*-test (two-tailed) $*P \leq 0.05$, $**P \leq 0.01$ (E–L).

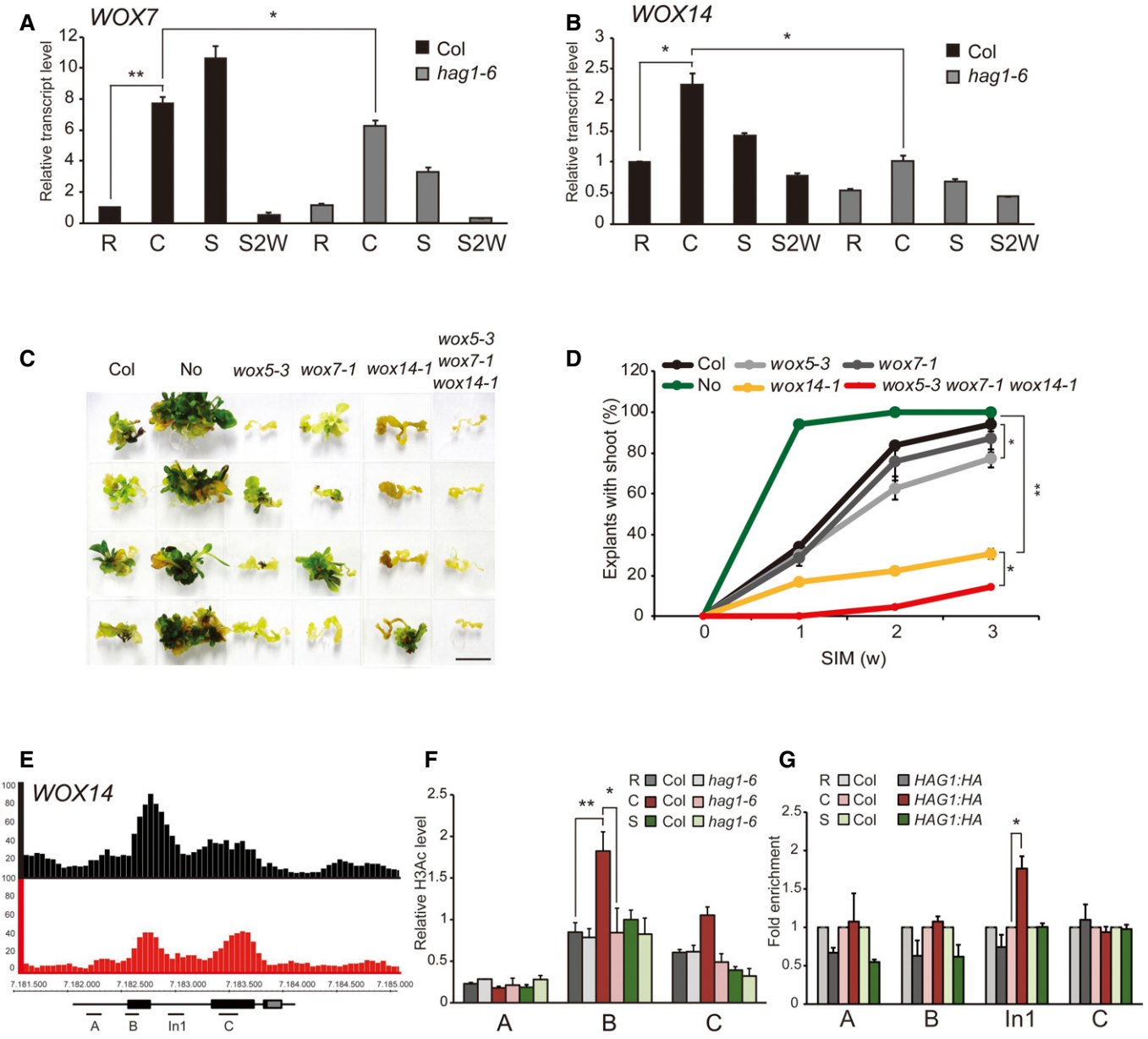

Figure 4. HAG1-regulated *WOX5*, *WOX7*, and *WOX14* are essential for *de novo* shoot regeneration.

A, B Transcript levels of *WOX7* (A) and *WOX14* (B) in Col and *hag1-6* roots (R), 4-day CIM explants (C), 4-day CIM + 2-day SIM explants (S), and 4-day CIM + 2-week SIM explants (S2W). Levels of Col R were set to 1 after normalization with *UBQ10*.

C, D *De novo* shoot regeneration of Col, Nossen (No), *wox5-3*, *wox7-1*, *wox14-1*, and *wox5-3 wox7-1 wox14-1* root explants. Col is the WT control for *wox5-3* and *wox7-1*, whereas No is the WT control for *wox14-1*. The picture was taken at 3 weeks on SIM using representative explants of each genotype. Scale bar: 1 cm. Percentage of explants with shoots was scored at indicated weeks on SIM (D).

E H3Ac enrichment at the *WOX14* locus in Col (upper black diagram) or *hag1-6* (lower red diagram) calli as determined by ChIP-seq. *P*-value cutoff for peak detection using MACS2 was 1 e^{-5}. See Fig 3A–D for schematic.

F ChIP-qPCR analysis of H3Ac levels at the *WOX14* locus of Col and *hag1-6*. Regions tested are indicated in the schematic in (E). Sample preparation and data presentation were performed as described in Fig 3E–H.

G Direct targeting of HAG1:HA protein to *WOX14* chromatin as determined by ChIP-qPCR. Regions tested are indicated in the schematic in (E). See Fig 3I–L for sample preparation and data presentation.

Data information: In (A, B, D, F, and G), data are presented as means ± SE. In (A, B, F, and G), three biological replicates were used for statistical analysis. Student's *t*-test (two-tailed) $*P \leq 0.05$, $**P \leq 0.001$. In (D), $n = 168$ for Col, 168 for No, 89 for *wox5-3*, 106 for *wox7-1*, 168 for *wox14-1*, and 168 for *wox5-3 wox7-1 wox14-1*.

mutants: the *scr-3* with a premature nonsense mutation and the *scr-6* with a T-DNA insertion (Appendix Fig S8A). Compared to the previously reported *scr-3* (Fukaki *et al*, 1996), the *scr-6* mutants displayed more severe phenotypes including smaller plant size and arrested root growth (Appendix Fig S8B). In correlation with the severity of the plant phenotypes, *de novo* shoot regeneration was partially impaired

in *scr-3*, whereas it was completely abolished in *scr-6* (Fig 5A–C and Appendix Fig S8C). To test the genetic relationship between *WOX5* and *SCR*, we generated the *wox5-3 scr-3* double mutant and evaluated it in a shoot-regeneration assay. *De novo* shoot regeneration as well as primary root growth was more severely impaired in *wox5-3 scr-3* compared to each single mutant (Fig 5D–F and Appendix Fig S8D and E). In concordance with the phenotypes, transcript levels of *PLT1* and *PLT2* in calli were also additively reduced by the combination of the *wox5-3* and *scr-3* mutations (Fig 5G and H). Thus, *WOX5* and *SCR* have additive roles in *de novo* shoot regeneration.

Activation of WOX5 and SCR rescues the shoot-regeneration defect of *hag1* and enhances shoot regeneration in WT

As another way to test whether *WOX5* and *SCR* might act as key factors conferring shoot-regeneration competence at the downstream of HAG1, we introgressed the dexamethasone (DEX)-inducible *35S::GVG-WOX5* (Sarkar *et al*, 2007) and/or *UBI::mCHERRY-GR-SCR* into WT and *hag1-6* (Appendix Fig S9A–D). Activation of WOX5 and SCR by DEX treatment resulted in agravitropic root growth and reduced primary root length in seedlings (Appendix Fig S10A and B). In addition, extra supernumerary layers of small columella cells in the root tip were observed (Appendix Fig S10C and D) as was previously reported for the DEX-treated *35S::GVG-WOX5* seedlings (Sarkar *et al*, 2007; Pi *et al*, 2015).

We then assayed for shoot-regeneration phenotypes upon activation of WOX5 and/or SCR in WT and *hag1-6* (Fig 6 and Appendix Fig S11A). Activation of WOX5 alone by DEX treatment induced the formation of pale leaf-like structures on *hag1* calli which seemed to be unable to develop into well-developed shoots (Fig 6A and B, and Appendix Fig S11B and C). On the other hand, *de novo* shoots were more efficiently regenerated by the activation of SCR (Fig 6C and D, and Appendix Fig S11C). Furthermore, the simultaneous activation of both WOX5 and SCR resulted in the higher percentage formation of trichome-bearing leaves, suggesting that the regenerated shoots have terminally differentiated epidermal cells (Fig 6E and F, and Appendix Fig S11C). These results indicate that the inactivation of *WOX5* and *SCR* is a major cause for the shoot-regeneration defect of *hag1*.

Interestingly, for the better rescue of the shoot-regeneration defect of *hag1*, WOX5 and SCR were required to be activated during early SIM incubation period or during both CIM and SIM incubation periods (Fig 6E and F, and Appendix Fig S11C), which is in line with the observation that the expression of *WOX5* and *SCR* was maintained throughout CIM and early SIM incubation periods (Fig 2A and B, and Appendix Fig S3A and B). However, a prolonged activation of WOX5 and SCR on SIM alone or on both CIM and SIM caused the inhibition rather than activation of shoot regeneration (Appendix Fig S12A–C). This inhibition was most prominent when both WOX5 and SCR were activated for long periods on both CIM and SIM (Appendix Fig S12A and B), indicating that their induction on SIM should be restricted to the initial periods of SIM for successful *de novo* shoot regeneration. Importantly, the activation of SCR alone or WOX5 and SCR together resulted in obviously enhanced shoot-regeneration efficiencies in WT Col background as well (Appendix Fig S13A and B). Therefore, WOX5 (with functional redundancy with WOX7/14) and SCR are believed to be key potency factors conferring regenerative competence to callus.

Discussion

Recent studies on global gene-expression profile during callus induction have substantiated the view of callus as lateral root-meristem-like tissue rather than embryo-like tissue (Sugimoto *et al*, 2010; this study). Thus, it is now generally accepted that callus formation may share a common pathway with lateral root initiation. However, the molecular regulatory pathway of cellular reprogramming occurring during callus formation and the molecular and cellular basis of pluripotency of callus cells remain obscure. In this study, we demonstrate that the *Arabidopsis* homolog of GCN5, AtGCN5/HAG1, is involved in cellular reprogramming in callus and essential for *de novo* shoot regeneration (Fig 7). Specifically in developing calli, HAG1 protein is induced and targeted to a group of genes including several root-meristem regulators such as *WOX5, WOX14, SCR, PLT1,* and *PLT2*. HAG1 mediates epigenetic changes at these root-meristem gene loci through histone acetylation and drives their transcriptional activation. We further demonstrate that WOX5, WOX14, and SCR, the downstream targets of HAG1, are also essential for conferring regeneration competence to callus cells by showing severely defective shoot-regeneration abilities of their mutant calli. Therefore, WOX5, WOX14, and SCR are crucial for the acquisition of regenerative competence, which is subsequently required for *de novo* shoot regeneration.

A stunning finding from mammalian stem cell studies was that pluripotent stem cells can be induced from differentiated somatic cells by the expression of only four key transcription factors, the OSKM (OCT4, SOX2, KLF4, and MYC; Takahashi & Yamanaka, 2006). Although the identity of such pluripotency factors in plants is yet to be confirmed through extensive and rigorous experiments as performed for iPS cells, our results suggest that WOXs and SCR might have similar roles in plant cells to the OSKM in mammalian cells. The rescue of the shoot-regeneration defect of *hag1* and the enhancement of the shoot-regeneration efficiency in WT by WOX5 and SCR activation reinforce such possibility.

Recently, it was proposed that *de novo* shoot organogenesis from plant explants maybe achieved by two distinct steps: acquisition of competence by the activation of root-meristem regulators and the completion of shoot regeneration by the upregulation of shoot-promoting factors (Kareem *et al*, 2015). In this view, HAG1 seems to play a major role in the first step. However, for the best rescue of the shoot-regeneration defect of *hag1* and the enhancement of shoot-regeneration efficiency in WT, the HAG1-dependent WOX5 and SCR activity seems to be required during early SIM incubation period or during both CIM and SIM incubation periods. This result suggests that the root-meristem regulators might have a yet-to-be characterized additional role on early SIM in addition to the role in cellular reprogramming on CIM. In line with this idea, on SIM, *hag1*-mutant calli showed no defect in the upregulation of shoot-promoting factor genes such as *CUC2* and *WUS*, whereas the spatial expression domain of *WUS* was severely altered in the *hag1-6* mutant. Therefore, one possibility is that the root-meristem regulators might direct the expression of the shoot-meristem genes into correct spatial domains during the initial stages of shoot-progenitor formation on SIM. Later on the root-meristem genes should have to be turned off as their prolonged activation on SIM clearly inhibited shoot regeneration.

It is notable that *hag1* and the mutants of the root-meristem regulators are capable of forming calli despite their inability to produce

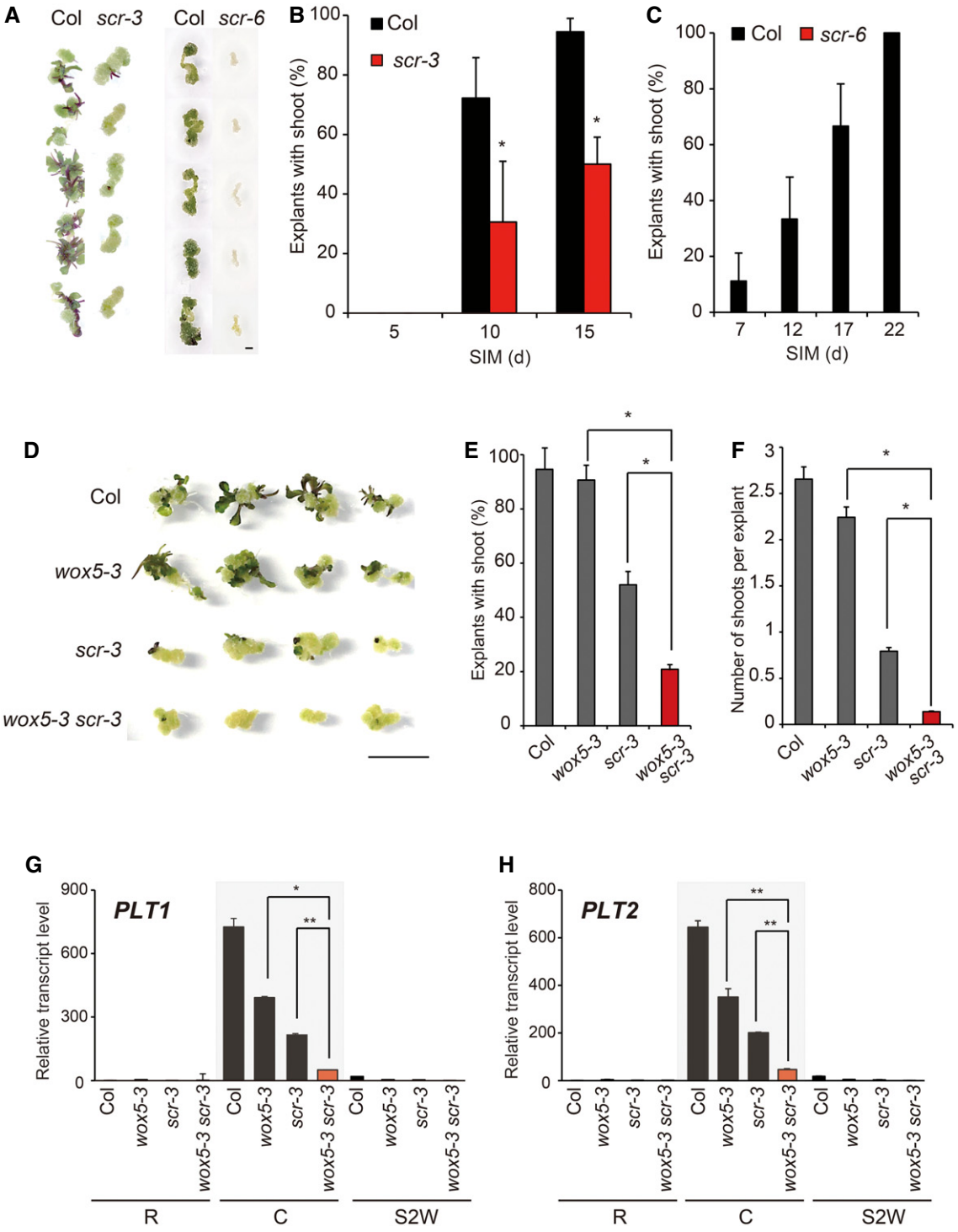

Figure 5. Mutations in *SCR* cause severe defects in *de novo* shoot regeneration.

A–C *De novo* shoot regeneration using Col and *scr* mutants; *scr-3* (A and B) and *scr-6* (A and C). Explants with shoots were scored at indicated days on SIM using Col and *scr-3* root explants that had been pre-incubated on CIM for 2 weeks (B) or Col and *scr-6* hypocotyl explants that had been pre-incubated on CIM for 1 week (C). Scale bar: 1 mm.

D–F *De novo* shoot regeneration of Col, *wox5-3*, *scr-3*, and *wox5-3 scr-3*. The percentage of root explants with shoots (E) and the number of shoots per root explant (F) were scored at 15 days on SIM. The explants had been pre-incubated on CIM for 2 weeks before transfer onto SIM. Scale bar: 1 cm.

G, H Transcript levels of *PLT1* (G) and *PLT2* (H) in Col, *wox5-3*, *scr-3*, and *wox5-3 scr-3* roots (R), 1-week CIM explants (C), and 1-week CIM + 2-week SIM explants (S2W) as determined by RT–qPCR. Levels of Col R were set to 1 after normalization with *UBQ10*.

Data information: In (B, C, and E–H), data are presented as means ± SE. In (G and H), three biological replicates were used for statistical analysis. Student's *t*-test (two-tailed) $*P \leq 0.001$, $**P \leq 0.05$. $n = 36$ (B), 14 (C), and 37 (E and F).

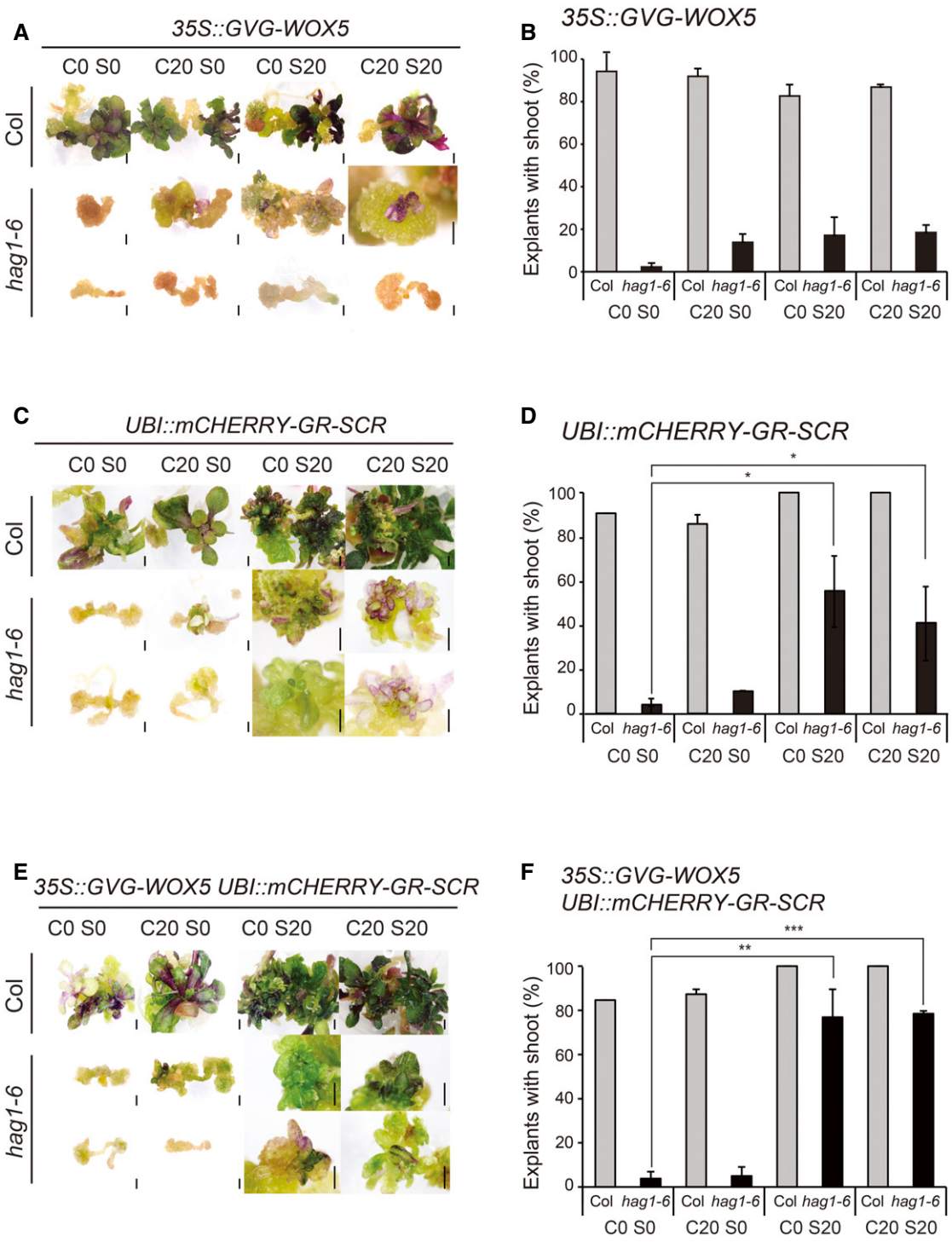

Figure 6. Activation of WOX5 and SCR rescues the shoot-regeneration defect of *hag1*.

A, B Activation of WOX5 by DEX treatment of *35S::GVG-WOX5* in Col and *hag1-6*. Root explants of *35S::GVG-WOX5* and *35S::GVG-WOX5 hag1-6* were transferred onto the indicated combinations of CIM and SIM supplemented with or without 20 μM DEX. DEX was treated for 3-day pulse period on CIM or/and SIM (see Materials and Methods for details and Appendix Fig S11A for schematics of the experimental procedure). Morphology of shoots regenerated from *35S::GVG-WOX5* and *35S::GVG-WOX5 hag1-6* root explants (A). Explants with shoots were scored at 3 weeks after transfer onto SIM with or without DEX (B).

C, D Activation of SCR by DEX treatment of *UBI::mCHERRY-GR-SCR* in Col and *hag1-6*. Sample preparation and data presentation are as described in (A and B).

E, F Activation of WOX5 and SCR by DEX treatment of *35S::GVG-WOX5 UBI::mCHERRY-GR-SCR* in Col and *hag1-6*. Sample preparation and data presentation are as described in (A and B).

Data information: Scale bars: 1 mm (A, C, and E). In (B, D, and F), data are presented as means ± SE. Student's *t*-test (two-tailed) $*P \leq 0.05$, $**P \leq 0.01$, $***P \leq 0.005$. $n > 42$ (B), $n > 33$ (D), and $n > 26$ (F) for each genotype and treatment.

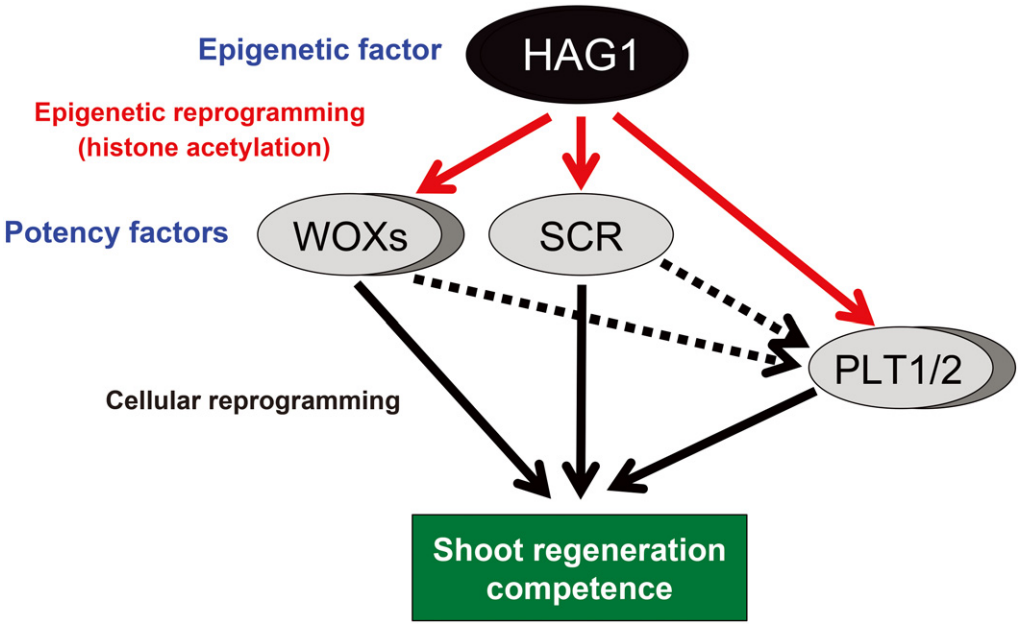

Figure 7. The HAG1-WOX5/WOX14/SCR/PLT1/PLT2 pathway is required for the acquisition of regenerative competence during *de novo* shoot regeneration.
Upon callus induction, HAG1 mediates epigenetic reprogramming of *WOX5*/*WOX14*, *SCR*, and *PLT1*/*PLT2* by catalyzing histone H3 acetylation at their chromatin. This epigenetic control on CIM assures the proper induction of these root transcription factors that act as potency factors establishing competence to regenerate shoots on SIM.

shoots. These features indicate that callus formation is a separate process from the acquisition of pluripotency and HAG1-regulated factors might be essential for converting noncompetent callus cells into reprogrammed competent cells instead of callus proliferation itself. Indeed, it is a well-known problem in the field of plant regeneration that long-term cultured calli generally lose competence for shoot organogenesis (Gould, 1986; Halperin, 1986; Bhojwani & Razdan, 1996), although underlying causes for it are largely unknown. Therefore, it might be interesting to study whether the root-meristem regulators are related with the loss-of-competence problem and their induced expression might solve it.

Together with HAG1, a variety of factors affecting root development and root stem cell maintenance, such as PLT1, PLT2, PLT3, PLT5, PLT7, LATERAL ORGAN BOUNDARIES DOMAIN 16 (LBD16), LBD17, LBD18, LBD29, AUXIN RESPONSE FACTOR 7 (ARF7), ARF9, ARF10, ARF19, SOLITARY ROOT (SLR), and PROPORZ 1 (PRZ1), are also known to be required for proper callus formation and/or shoot regeneration (Sieberer *et al*, 2003; Sugimoto *et al*, 2010; Fan *et al*, 2012; Qiao *et al*, 2012; Ikeuchi *et al*, 2013; Kareem *et al*, 2015; Liu *et al*, 2016; Shang *et al*, 2016). These and our own findings lead us to speculate if there is a general correlation between callus-forming activity and the capacity of shoot regeneration from callus. In some cases, such as *slr* mutants (Shang *et al*, 2016) and suppressors of multiple *LBDs* (Fan *et al*, 2012), compromised shoot-regeneration capacities are likely direct outcomes from defects in callus formation. In other cases, such as *prz1* (Sieberer *et al*, 2003), *plt3 plt5 plt7* (Kareem *et al*, 2015), *hag1*, and *wox5-3 scr-3* mutants (this study), calli displaying uncompromised proliferation activities show severely defective shoot-regeneration capacities. In the case of *lbd16-2* mutants that are defective in shoot regeneration (Fan *et al*, 2012; Liu *et al*, 2018), loss of root cell-like identity and reduced cell division activity are both observed in the callus. Therefore, root-development regulators seem to play diverse rather than common roles during callus formation and the establishment of regenerative potential. As *de novo* shoot regeneration involves multiple steps, including callus initiation, callus proliferation, establishment of shoot-meristem progenitor, and shoot patterning, each root-development regulator might act at one or multiples steps of this process.

One critical question is how root-meristem regulators including WOXs and SCR contribute to the acquisition of regenerative competence in callus. Perhaps recent studies on the role of WOX5 and SCR in the patterning of root stem cell niche might provide a hint for their roles as pluripotency factors. WOX5 has been reported to repress the differentiation of stem cells (Sarkar *et al*, 2007; Pi *et al*, 2015). WOX5 protein diffuses from the QC to the columella stem cells and represses their differentiation by establishing and maintaining the gradient of CDF4, a differentiation factor, across the root stem cell niche through chromatin-mediated repression of *CDF4* expression (Pi *et al*, 2015). Notably, the ectopic expression of WOX5 in columella cells converts already differentiated columella cells into stem cell-like cells showing that WOX5 has a cell-reprogramming potential. WOX5 is also known to act redundantly with other root-meristem maintenance factors including SCR and PLTs to repress ectopic differentiation in the root meristem, suggesting that they, as transcription factors, might regulate overlapping target genes (Sarkar *et al*, 2007; Tucker & Laux, 2007). Another study reported that SCR represses cytokinin-dependent cell differentiation in the root stem cell niche by directly repressing *ARR1*, a gene encoding cytokinin-responsive differentiation-promoting factor (Moubayidin *et al*, 2013). Therefore, as in roots and mammalian systems (Jopling *et al*, 2011; Liang & Zhang, 2013), repression of differentiated cell traits and induction of competence for differentiation might also be prerequisites to acquire pluripotency in callus. During callus formation, WOXs and SCR might act as master regulators in establishing and maintaining

cellular regenerative competence, and possibly pluripotency, by repressing factors that in turn would promote differentiation.

Materials and Methods

Plant materials

The *Arabidopsis thaliana* accessions Colombia-0 (Col) and Nossen (No) were used in this study. *hag1-6* (SALK_150784), *hag1-7* (SALK_106557), *wox7-1* (SALK_065801), *scr-3* (CS3997), and *scr-6* (SALK_032192) are all in the Col background and were obtained from TAIR (http://www.arabidopsis.org). *wox14-1* (pst13645), which is in the No background, was obtained from RIKEN (http://www.brc.riken.jp/lab/epd/Eng). *wox5-1*, *wox5-3*, and *35S::GVG-WOX5* were kind gifts from Thomas Laux (Universtät Freiburg, Germany). *pWOX::GFP-ER* and *pWUS::mGFP-ER* were provided by Elliot M. Meyerowitz (Caltech, USA), and *pSCR::GFP-ER* and *CYCB1;1:GUS* were provided by Philip Benfey (Duke University, USA) and Peter Doerner (University of Edinburgh, UK), respectively. Each transgenic line was crossed with plants heterozygous for *hag1-6* mutation. F3 progeny homozygous for the transgenes and *hag1-6* mutation were used for experiments. *wox5-3 scr-3* double mutant and *wox5-3 wox7-1 wox14-1* triple mutants were generated through genetic crosses.

Growth conditions

Seeds were germinated on Murashige and Skoog (MS) medium supplemented with 1% sucrose and buffered to pH 5.7 with 0.05% MES. Plants were grown under 100 μmol/m^2/s cool white fluorescent lights at 22°C in long days with a 16-h light and 8-h dark photoperiod.

Constructs and plant transformation

Construction details of the *35S::FLAG:HAG1* were previously described (Kim *et al*, 2015). *35S::FLAG:HAG1* was transformed into heterozygous *hag1-7* plants via *Agrobacterium*-mediated transformation using floral dip method (Clough & Bent, 1998). Homozygous transgenic *35S::FLAG:HAG1 hag1-7* plants were selected in the subsequent generations through genotyping.

To generate *HAG1:HA*, a genomic *HAG1* fragment including the 1.151 kb promoter region upstream of the start codon was amplified using HAG1 genomic entry-F (5′-CACCAGTTAAAACTGAAGCC GAACCA-3′) and HAG1 genomic entry-R (5′-TTGAGATTTAGCAC CAGATTGGAG-3′) primers, cloned first into pENTR™/SD/D-TOPO entry vector (Invitrogen), and subsequently subcloned into pEarleyGate301 destination vector (Earley *et al*, 2006). *HAG1:HA* was transformed into heterozygous *hag1-6* via *Agrobacterium*-mediated transformation using floral dip method (Clough & Bent, 1998). Homozygous transgenic *HAG1:HA hag1-6* plants were selected in the subsequent generations. *UBI::mCHERRY-GR-SCR* was generated in two steps. First *UBI::mCHERRY-GR-linker-WUS:TrbcS* construct, plasmid pJF359, was generated via a Gateway™ LR reaction. The destination vector was pFK273 which is based on pGreenIIS (Hellens *et al*, 2000; Mathieu *et al*, 2007). It provided the promoter and terminator sequences and a BASTA (glufosinate-ammonium) resistance cassette. The entry vector, plasmid pJF355, is based on pENTR1A and contains the mCHERRY-GR-linker-WUS coding sequence. Second, the coding sequence of *SCR* was amplified using SCR_CDS_SalIF (5′-TTTGTCGACATGGCGGAATCCGGCGATTTCA AC-3′) and SCR_CDS_SacIR (5′-TTTGAGCTCCTAAGAACGAGGCG TCCAAGCAG-3′) primers and cloned first into the 35S-pPZP221-RbcS vector (Choi *et al*, 2012). Then, the *SCR* coding sequence and the Rubisco small subunit (RbcS) terminator were amplified using SCR_NOT1-F (5′-TTTGCGGCCGCTATGGCGGAATCCGGCGATTTCA AC-3′) and SCR_RbcS_MfeI-R (5′-TTTCAATTGCAAACATATAGTA GATGCGACG-3′) primers and subcloned into the *UBI::mCHERRY-GR-linker-WUS:TrbcS* by removing the *WUS* coding sequence and the RbcS terminator with NotI and MfeI digestion and replacing them with the *SCR* coding sequence and the RbcS terminator. *UBI::mCHERRY-GR-SCR* was transformed into heterozygous *hag1-6*. Homozygous transgenic *UBI::mCHERRY-GR-SCR hag1-6* plants were selected in the subsequent generations through selection and genotyping. *35S::GVG-WOX5 UBI::mCHERRY-GR-SCR* in Col and *hag1-6* backgrounds were generated by crossing *35S::GVG-WOX5* in heterozygous *hag1-6* with *UBI::mCHERRY-GR-SCR* in heterozygous *hag1-6* and genotyping progenies of subsequent generations.

Culture conditions

For callus induction, root-, cotyledon-, or hypocotyl-derived explants from 2-week- to 20-day-old seedlings were excised, transferred onto CIM, and cultured in the dark. Unless otherwise noted, the composition of CIM used in this study contains Gamborg's B5 medium with minimal organics (Sigma-Aldrich), 3% sucrose buffered to pH 5.7 with 0.05% MES, and 0.8% phytoagar supplemented with 0.5 mg/l 2,4-dichlorophenoxyacetic acid (2,4-D) and 0.1 mg kinetin. For shoot regeneration, root-derived explants incubated on CIM for 7 days were transferred onto SIM and incubated under continuous fluorescent light at 22°C. SIM is consisted of Gamborg's B5 medium with minimal organics (Sigma-Aldrich), 3% sucrose buffered to pH 5.7 with 0.05% MES, and 0.8% phytoagar supplemented with 158 mg/l indole-3-acetic acid (IAA) and 894 mg/l N^6-(2-isopentenyl)adenine (2IP). For *de novo* root organogenesis, root-derived explants placed on CIM for 7 days were transferred onto RIM and incubated under continuous dark at 22°C. The composition of RIM was identical to that of SIM except for 158 mg/l of IAA without 2IP. Regenerated shoots or roots were scored at indicated days after transfer onto the corresponding medium. For dexamethasone (DEX, Sigma-Aldrich) treatment, root explants were transferred onto CIM with 20 μM DEX (C20) or CIM without DEX (C0). After 3 days of induction on either C20 or C0, tissues were washed three times with sterile water to remove residual DEX. Then, explants were placed on fresh, DEX-free CIM. After 7 days, both C20 and C0 explants were placed on either SIM supplemented with DEX (S20) or without DEX (S0). After 3 days on S20 and S0, tissues were washed three times with sterile water to remove residual DEX and transferred onto fresh SIM for shoot regeneration.

Microscopy

50 μg/ml of propidium iodide (PI) was used for counterstaining of the cell outlines. Images were observed with confocal laser microscope (Carl Zeiss LSM700). At least 20 explants were observed and imaged to infer the representative pattern of each sample.

Quantification of GFP-signal intensity was performed by using Adobe Photoshop.

Immunoblot analysis

Total protein was extracted using protein extraction buffer (50 mM Tris–HCl pH 7.5, 150 mM NaCl, 10 mM $MgCl_2$, 5 mM EDTA, 0.6 mM PMSF, 80 μM MG132, proteinase inhibitor cocktail, and 10% glycerol). Protein samples were quantified using a protein assay kit (Bio-Rad), and 30 μg was subjected to Western blot analysis. Anti-HA antibody (Abcam ab9110) was used at 1:3,000 dilution for the detection of HAG1:HA protein.

Histochemical GUS assay

GUS staining was performed as described (Han *et al*, 2007). At least 30 root-derived explants were stained for each genotype to infer the representative pattern of each sample. Images were observed with stereomicroscope (Carl Zeiss STEM2000). Quantification of GUS-staining intensity was performed by using Image J (Béziat *et al*, 2017).

RNA-seq analysis

Col and *hag1-6* roots (R), 4-day CIM-incubated (C), 4-day CIM-incubated + 2-day SIM-incubated (S), and 4-day CIM-incubated + 2-week SIM-incubated (S2W) root explants were collected for the assay. Total RNA was isolated using TRI Reagent (MRC) and purified with RNeasy Mini Kit (QIAGEN) to have an $OD_{260/280}$ ratio of 1.8–2.2. Library preparation and sequencing via Illumina HiSeq™ 2000 was performed by Beijing Genomics Institute (Hong Kong). Clean reads were mapped to the Col genomic sequence (http://1001genomes.org/accessions.html) using SOAP aligner/soap2, and mismatches with no more than 2 bases were allowed in the alignment. Unless stated otherwise, differentially expressed genes (DEGs) were selected with FDR ≤ 0.001 and $|\log_2 \text{ratio}| \geq 1$ as thresholds.

RT–qPCR analysis

3 μg of total RNA was reverse-transcribed using M-MuLV reverse transcriptase (Fermentas) and oligo (dT) primer. Following reverse transcription (RT), quantitative PCR (qPCR) was performed on first-strand DNA with real-time PCR cycler (QIAGEN Rotor Gene Q) by using SYBR Green I master mix (Kappa). Quantification using standard curves was performed to determine the amount of target genes in each sample. The transcript levels of each gene were normalized to the level of the internal control, *Ubiquitin 10* (*UBQ10*). The experiments were repeated at least three times for each gene. Gene-specific primers used for RT–qPCR analyses are as listed in Table EV3.

ChIP-qPCR analysis

ChIP assays against H3Ac and HA were performed as previously described (Johnson *et al*, 2002; Han *et al*, 2007) using anti-H3Ac (Millipore 06-599) and anti-HA (Abcam ab9110) antibodies. For ChIP binding assays, β-glycerophosphate, sodium fluoride, and MG132 were added to all extraction and lysis buffers. The amount of immunoprecipitated DNA was quantified by qPCR as described in the above section. Relative amounts of each amplified product were determined by using the comparative $\Delta\Delta C_T$ method (Livak & Schmittgen, 2001). The amount of immunoprecipitated DNA was normalized to the respective input DNA (DNA isolated from chromatin that was cross-linked and fragmented under the same conditions as the immunoprecipitated DNA) and the corresponding control sample. The fold enrichment was calculated by comparing the normalized value of each fragment to that of *UBQ11*. For ChIP binding assays, levels of nontransgenic control roots (R) were set to 1 after normalization to the levels of the input DNA. Primers used for ChIP-qPCR analyses are listed in Table EV3.

ChIP-seq analysis

ChIP using anti-H3Ac antibody (Millipore 06-599) was performed as previously described (Han *et al*, 2007; Kim *et al*, 2015) except that protein agarose A beads (Santa Cruz 2001) were used instead of salmon sperm DNA/Protein A agarose beads (Upstate 16-157). Input or ChIPed DNA was eluted with 12 μl distilled water using MinElute PCR Purification Kit (QIAGEN), and 2 μl of it was used for quantification using Qubit 2.0 Fluorometer (Life Technologies). Part of sample was also used for qPCR analysis to validate the enrichment patterns of known loci. At least 12 ng of input or ChIPed DNA was pooled from seven independent experiments, and its quality was assessed with 2100 (Agilent) and Lab ChIP GX (Caliper). Further procedures including DNA-end repair, adaptor ligation, amplification, construction of sequencing library, and sequencing using Illumina HiSeq™ 2000 were performed by Beijing Genomics Institute (Hong Kong). Sequenced reads were mapped to the reference genome of Col, and only uniquely mapped reads were selectively and used for analysis. Gene depth distributions of the uniquely mapped reads were obtained by BEDTools (http://bedtools.readthedocs.io/en/latest/). Aligned reads were analyzed using Model-based Analysis for ChIP-seq (MACS) (Zhang *et al*, 2008) to further analyze regions enriched with H3Ac peaks after normalization to the respective input DNA using *P*-value cutoff of $1e^{-5}$ or $5e^{-2}$. Annotation of peaks was performed using HOMER v4.9 (http://homer.ucsd.edu/homer/) and visualized using Integrated Genome Browser (IGB; http://bioviz.org/igb/index.html). Identification of differential peaks between Col and *hag1-6* samples was performed using MAnorm (Shao *et al*, 2012) and MACS2 bdgdiff (Feng *et al*, 2012). Statistical details of experiments are included in Figures, Figure legends, Dataset legends, and Appendix Figure legends.

Data availability

Data for RNA-seq and ChIP-seq analyses have been deposited into Gene Expression Omnibus (http://www.ncbi.nlm.nih.gov/geo/) and are accessible through accession number GSE100967 which is comprised of SubSeries accession numbers GSE100965 and GSE100966.

Expanded View for this article is available online.

Acknowledgements

We thank EM Meyerowitz for sharing *pWOX5::GFP-ER* and *pWUS::GFP-ER*. *35S::GVG-WOX5*, *wox5-1*, and *wox5-3* were kindly provided by T Laux. We also thank

P Benfey and P Doerner for sharing *pSCR::GFP-ER* and *CYCB1;1:GUS*, respectively. We are grateful to Segun Goh for his help with analyzing ChIP-seq data. This work was supported by a grant from the National Research Foundation of Korea (NRF) (NRF-2016R1A2A1A05005477).

Author contributions

J-YK, BN, and Y-SN conceptualized the study; J-YK, BN, and Y-SN designed the experiments; J-YK and WY performed the experiments; J-YK, WY, BN, and Y-SN analyzed the data; JF and JUL provided critical materials; J-YK, BN, and Y-SN wrote the manuscript.

Conflict of interest

The authors declare that they have no conflict of interest.

References

Aida M, Beis D, Heidstra R, Willemsen V, Blilou I, Galinha C, Nussaume L, Noh YS, Amasino R, Scheres B (2004) The PLETHORA genes mediate patterning of the *Arabidopsis* root stem cell niche. *Cell* 119: 109 – 120

Atta R, Laurens L, Boucheron-Dubuisson E, Guivarc'h A, Carnero E, Giraudat-Pautot V, Rech P, Chriqui D (2009) Pluripotency of *Arabidopsis* xylem pericycle underlies shoot regeneration from root and hypocotyl explants grown *in vitro*. *Plant J* 57: 626 – 644

Béziat C, Kleine-Vehn J, Feraru E (2017) Histochemical staining of beta-glucuronidase and its spatial quantification. *Methods Mol Biol* 1497: 73 – 80

Bhojwani SS, Razdan MK (1996) Somatic embryogenesis. In *Plant tissue culture: theory and practice, a revised edition. Amsterdam, Elsevier*, Bhojwani SS, Razdan MK (eds), pp 125 – 166. Oxford: Oxford University Press

Bonnet J, Wang CY, Baptista T, Vincent SD, Hsiao WC, Stierle M, Kao CF, Tora L, Devys D (2014) The SAGA coactivator complex acts on the whole transcribed genome and is required for RNA polymerase II transcription. *Genes Dev* 28: 1999 – 2012

Choi SM, Song HR, Han SK, Han M, Kim CY, Park J, Lee YH, Jeon JS, Noh YS, Noh B (2012) HDA19 is required for the repression of salicylic acid biosynthesis and salicylic acid-mediated defense responses in *Arabidopsis*. *Plant J* 71: 135 – 146

Christen B, Robles V, Raya M, Paramonov I, Izpisua Belmonte JC (2010) Regeneration and reprogramming compared. *BMC Biol* 8: 5

Clough SJ, Bent AF (1998) Floral dip: a simplified method for *Agrobacterium*-mediated transformation of *Arabidopsis thaliana*. *Plant J* 16: 735 – 743

Colón-Carmona A, You R, Haimovitch-Gal T, Doerner P (1999) Technical advance: spatio-temporal analysis of mitotic activity with a labile cyclin-GUS fusion protein. *Plant J* 20: 503 – 508

Denis E, Kbiri N, Mary V, Claisse G, Conde E, Silva N, Kreis M, Deveaux Y (2017) WOX14 promotes bioactive gibberellin synthesis and vascular cell differentiation in *Arabidopsis*. *Plant J* 90: 560 – 572

Deveaux Y, Toffano-Nioche C, Claisse G, Thareau V, Morin H, Laufs P, Moreau H, Kreis M, Lecharny A (2008) Genes of the most conserved WOX clade in plants affect root and flower development in *Arabidopsis*. *BMC Evol Biol* 8: 291

Earley KW, Haag JR, Pontes O, Opper K, Juehne T, Song K, Pikaard CS (2006) Gateway-compatible vectors for plant functional genomics and proteomics. *Plant J* 45: 616 – 629

Etchells JP, Provost CM, Mishra L, Turner SR (2013) WOX4 and WOX14 act downstream of the PXY receptor kinase to regulate plant vascular proliferation independently of any role in vascular organisation. *Development* 140: 2224 – 2234

Fan M, Xu C, Xu K, Hu Y (2012) Lateral organ boundaries domain transcription factors direct callus formation in *Arabidopsis* regeneration. *Cell Res* 22: 1169 – 1180

Feng J, Liu T, Qin B, Zhang Y, Liu XS (2012) Identifying ChIP-seq enrichment using MACS. *Nat Protoc* 7: 1728 – 1740

Fukaki H, Fujisawa H, Tasaka M (1996) *SGR1*, *SGR2*, *SGR3*: novel genetic loci involved in shoot gravitropism in *Arabidopsis thaliana*. *Plant Physiol* 110: 945 – 955

Gallois JL, Woodward C, Reddy GV, Sablowski R (2002) Combined SHOOT MERISTEMLESS and WUSCHEL trigger ectopic organogenesis in *Arabidopsis*. *Development* 129: 3207 – 3217

Gallois JL, Nora FR, Mizukami Y, Sablowski R (2004) WUSCHEL induces shoot stem cell activity and developmental plasticity in the root meristem. *Genes Dev* 18: 375 – 380

Gaspar-Maia A, Alajem A, Meshorer E, Ramalho-Santos M (2011) Open chromatin in pluripotency and reprogramming. *Nat Rev Mol Cell Biol* 12: 36 – 47

Gordon SP, Heisler MG, Reddy GV, Ohno C, Das P, Meyerowitz EM (2007) Pattern formation during *de novo* assembly of the *Arabidopsis* shoot meristem. *Development* 134: 3539 – 3548

Gould AF (1986) Factors controlling generation of viability *in vitro*. In *Cell Culture and Somatic Cell Genetics of Plants*, Vasil IK (ed.), pp 549 – 567. New York: Academic Press

Halperin W (1986) Attainment and retention of morphogenic capacity *in vitro*. In *Cell Culture and Somatic Cell Genetics of Plants*, pp 3 – 47. Vasil IK (ed)New York: Academic Press

Han SK, Song JD, Noh YS, Noh B (2007) Role of plant CBP/p300-like genes in the regulation of flowering time. *Plant J* 49: 103 – 114

Hellens RP, Edwards EA, Leyland NR, Bean S, Mullineaux PM (2000) pGreen: a versatile and flexible binary Ti vector for *Agrobacterium*-mediated plant transformation. *Plant Mol Biol* 42: 819 – 832

Ikeuchi M, Sugimoto K, Iwase A (2013) Plant callus: mechanisms of induction and repression. *Plant Cell* 25: 3159 – 3173

Johnson LM, Cao XF, Jacobsen SE (2002) Interplay between two epigenetic marks: DNA methylation and histone H3 lysine 9 methylation. *Curr Biol* 12: 1360 – 1367

Jopling C, Boue S, Izpisua Belmonte JC (2011) Dedifferentiation, transdifferentiation and reprogramming: three routes to regeneration. *Nat Rev Mol Cell Biol* 12: 79 – 89

Kareem A, Durgaprasad K, Sugimoto K, Du Y, Pulianmackal AJ, Trivedi ZB, Abhayadev PV, Pinon V, Meyerowitz EM, Scheres B, Prasad K (2015) PLETHORA genes control regeneration by a two-step mechanism. *Curr Biol* 25: 1017 – 1030

Kim JY, Oh JE, Noh YS, Noh B (2015) Epigenetic control of juvenile-to-adult phase transition by the *Arabidopsis* SAGA-like complex. *Plant J* 83: 537 – 545

Kong D, Hao Y, Cui H (2016) The WUSCHEL related homeobox protein WOX7 regulates the sugar response of lateral root development in *Arabidopsis thaliana*. *Mol Plant* 9: 261 – 270

Kornet N, Scheres B (2009) Members of the GCN5 histone acetyltransferase complex regulate PLETHORA-mediated root stem cell niche maintenance and transit amplifying cell proliferation in *Arabidopsis*. *Plant Cell* 21: 1070 – 1079

Krebs AR, Karmodiya K, Lindahl-Allen M, Struhl K, Tora L (2011) SAGA and ATAC histone acetyl transferase complexes regulate distinct sets of genes and ATAC defines a class of p300-independent enhancers. *Mol Cell* 44: 410 – 423

Laux T, Mayer KF, Berger J, Jurgens G (1996) The WUSCHEL gene is required for shoot and floral meristem integrity in *Arabidopsis*. *Development* 122: 87 – 96

Ledford H (2016) Plant-genome hackers seek better ways to produce customized crops. *Nature* 539: 16 – 17

Lee TI, Causton HC, Holstege FC, Shen WC, Hannett N, Jennings EG, Winston F, Green MR, Young RA (2000) Redundant roles for the TFIID and SAGA complexes in global transcription. *Nature* 405: 701 – 704

Liang G, Zhang Y (2013) Embryonic stem cell and induced pluripotent stem cell: an epigenetic perspective. *Cell Res* 23: 49 – 69

Liu Z, Li J, Wang L, Li Q, Lu Q, Yu Y, Li S, Bai MY, Hu Y, Xiang F (2016) Repression of callus initiation by the miRNA-directed interaction of auxin-cytokinin in *Arabidopsis thaliana*. *Plant J* 87: 391 – 402

Liu J, Hu X, Qin P, Prasad K, Hu Y, Xu L (2018) The WOX11–LBD16 Pathway promotes pluripotency acquisition in callus cells during *de novo* shoot regeneration in tissue culture. *Plant Cell Physiol* 59: 734 – 743

Livak KJ, Schmittgen TD (2001) Analysis of relative gene expression data using real-time quantitative PCR and the $2^{-\Delta\Delta C}$T method. *Methods* 25: 402 – 408

Mathieu J, Warthmann N, Kuttner F, Schmid M (2007) Export of FT protein from phloem companion cells is sufficient for floral induction in *Arabidopsis*. *Curr Biol* 17: 1055 – 1060

Mayer KF, Schoof H, Haecker A, Lenhard M, Jurgens G, Laux T (1998) Role of WUSCHEL in regulating stem cell fate in the *Arabidopsis* shoot meristem. *Cell* 95: 805 – 815

Melcer S, Meshorer E (2010) Chromatin plasticity in pluripotent cells. *Essays Biochem* 48: 245 – 262

Meshorer E, Misteli T (2006) Chromatin in pluripotent embryonic stem cells and differentiation. *Nat Rev Mol Cell Biol* 7: 540 – 546

Motte H, Verstraeten I, Werbrouck S, Geelen D (2011) CUC2 as an early marker for regeneration competence in *Arabidopsis* root explants. *J Plant Physiol* 168: 1598 – 1601

Moubayidin L, Di Mambro R, Sozzani R, Pacifici E, Salvi E, Terpstra I, Bao D, van Dijken A, Dello Ioio R, Perilli S, Ljung K, Benfey PN, Heidstra R, Costantino P, Sabatini S (2013) Spatial coordination between stem cell activity and cell differentiation in the root meristem. *Dev Cell* 26: 405 – 415

Pandey R, Muller A, Napoli CA, Selinger DA, Pikaard CS, Richards EJ, Bender J, Mount DW, Jorgensen RA (2002) Analysis of histone acetyltransferase and histone deacetylase families of *Arabidopsis thaliana* suggests functional diversification of chromatin modification among multicellular eukaryotes. *Nucleic Acids Res* 30: 5036 – 5055

Pi L, Aichinger E, van der Graaff E, Llavata-Peris CI, Weijers D, Hennig L, Groot E, Laux T (2015) Organizer-derived WOX5 signal maintains root columella stem cells through chromatin-mediated repression of CDF4 expression. *Dev Cell* 33: 576 – 588

Sarkar AK, Luijten M, Miyashima S, Lenhard M, Hashimoto T, Nakajima K, Scheres B, Heidstra R, Laux T (2007) Conserved factors regulate signaling in *Arabidopsis thaliana* shoot and root stem cell organizers. *Nature* 446: 811 – 814

Servet C, Conde e Silva N, Zhou DX (2010) Histone acetyltransferase AtGCN5/HAG1 is a versatile regulator of developmental and inducible gene expression in *Arabidopsis*. *Mol Plant* 3: 670 – 677

Shang B, Xu C, Zhang X, Cao H, Xin W, Hu Y (2016) Very-long-chain fatty acids restrict regeneration capacity by confining pericycle competence for callus formation in *Arabidopsis*. *Proc Natl Acad Sci USA* 113: 5101 – 5106

Shao Z, Zhang Y, Yuan GC, Orkin SH, Waxman DJ (2012) MAnorm: a robust model for quantitative comparison of ChIP-Seq data sets. *Genome Biol* 13: R16

Sieberer T, Hauser MT, Seifert GJ, Luschnig C (2003) PROPORZ 1, a putative *Arabidopsis* transcriptional adaptor protein, mediates auxin and cytokinin signals in the control of cell proliferation. *Curr Biol* 13: 837 – 842

Skoog F, Miller CO (1957) Chemical regulation of growth and organ formation in plant tissues cultured *in vitro*. *Symp Soc Exp Biol* 11: 118 – 130

Stewart S, Stankunas K (2012) Limited dedifferentiation provides replacement tissue during zebrafish fin regeneration. *Dev Biol* 365: 339 – 349

Sugimoto K, Jiao Y, Meyerowitz EM (2010) *Arabidopsis* regeneration from multiple tissues occurs via a root development pathway. *Dev Cell* 18: 463 – 471

Takahashi K, Yamanaka S (2006) Induction of pluripotent stem cells from mouse embryonic and adult fibroblast cultures by defined factors. *Cell* 126: 663 – 676

Tucker MR, Laux T (2007) Connecting the paths in plant stem cell regulation. *Trends Cell Biol* 17: 403 – 410

Verdeil JL, Alemanno L, Niemenak N, Tranbarger TJ (2007) Pluripotent versus totipotent plant stem cells: dependence versus autonomy? *Trends Plant Sci* 12: 245 – 252

Vlachonasios KE, Thomashow MF, Triezenberg SJ (2003) Disruption mutations of ADA2b and GCN5 transcriptional adaptor genes dramatically affect *Arabidopsis* growth, development, and gene expression. *Plant Cell* 15: 626 – 638

Zhang Y, Liu T, Meyer CA, Eeckhoute J, Johnson DS, Bernstein BE, Nusbaum C, Myers RM, Brown M, Li W, Liu XS (2008) Model-based analysis of ChIP-Seq (MACS). *Genome Biol* 9: R137

Zhao J, Morozova N, Williams L, Libs L, Avivi Y, Grafi G (2001) Two phases of chromatin decondensation during dedifferentiation of plant cells: distinction between competence for cell fate switch and a commitment for S phase. *J Biol Chem* 276: 22772 – 22778

Zipori D (2004) The nature of stem cells: state rather than entity. *Nat Rev Genet* 5: 873 – 878

